Triplet Sensitizers

Deutsche Ausgabe: DOI: 10.1002/ange.201608442
Internationale Ausgabe: DOI: 10.1002/anie.201608442

Iridium(III) Complexes Bearing Pyrene-Functionalized 1,10-Phenanthroline Ligands as Highly Efficient Sensitizers for Triplet–Triplet Annihilation Upconversion

*Yue Lu, Junsi Wang, Niamh McGoldrick, Xiaoneng Cui, Jianzhang Zhao, Colin Caverly, Brendan Twamley, Gearoid M. Ó Máille, Bryan Irwin, Robert Conway-Kenny, and Sylvia M. Draper**

Abstract: *"Chemistry-on-the-complex" synthetic methods have allowed the selective addition of 1-ethynylpyrene appendages to the 3-, 5-, 3,8- and 5,6-positions of Ir^{III}-coordinated 1,10-phenanthroline via Sonogashira cross-coupling. The resulting suite of complexes has given rise to the first rationalization of their absorption and emission properties as a function of the number and position of the pyrene moieties. Strong absorption in the visible region (e.g. 3,8-substituted* ***Ir-3****: $\lambda_{abs} = 481$ nm, $\varepsilon = 52\,400\ M^{-1}cm^{-1}$) and long-lived triplet excited states (e.g. 5-substituted* ***Ir-2****: $\tau_T = 367.7\ \mu s$) were observed for the complexes in deaerated CH_2Cl_2. On testing the series as triplet sensitizers for triplet–triplet annihilation upconversion, those Ir^{III} complexes bearing pyrenyl appendages at the 3- and 3,8-positions (****Ir-1****,* ***Ir-3****) were found to give optimal upconversion quantum yields (30.2 % and 31.6 % respectively).*

Triplet–triplet annihilation (TTA) upconversion has attracted considerable attention in recent years due to its potential to demonstrate radical improvements in photovoltaics,[1–3] bioimaging,[4–6] and photocatalysis.[7,8] It is a light-driven process that involves the combination of two triplet excited state energies (from molecules acting as photosensitizer and acceptor) and an anti-Stokes delayed fluorescence from the singlet state of the carefully chosen annihilator. Effective triplet sensitizers for use in upconversion processes require efficient intersystem crossing (ISC), strong absorption in the visible region and relatively long-lived triplet excited state lifetimes.[9] While these criteria are widely recognized, the design of potential triplet sensitizers has proven to be a considerable challenge, requiring a more thorough understanding of the relationship between the photophysical properties and molecular structure of the photosensitizer.

[*] Y. Lu, J. Wang, Dr. N. McGoldrick, C. Caverly, Dr. B. Twamley, Dr. G. M. Ó Máille, B. Irwin, R. Conway-Kenny, Prof. Dr. S. M. Draper
Department of Chemistry, Trinity College Dublin
Dublin 2 (Ireland)
E-mail: smdraper@tcd.ie
X. Cui, Prof. Dr. J. Zhao
State Key Laboratory of Fine Chemicals
Dalian University of Technology
Dalian, 116024 (P. R. China)
Supporting information and the ORCID identification number(s) for the author(s) of this article can be found under http://dx.doi.org/10.1002/anie.201608442.

In recent years, Ir^{III} complexes have been investigated as triplet photosensitizers for TTA upconversion applications.[10–14] To date only limited numbers of literature examples exist that demonstrate the requisite intense visible light absorption and long excited-state lifetimes.[10,14,15] As a result an exciting opportunity remains for synthetic chemists to optimize the properties of Ir^{III} centers in a manner that furthers our understanding of and enhances their potential for use in, this field.

Herein, we report a family of novel cyclometalated Ir^{III} complexes based on 1,10-phenanthroline (phen). Each member of the family has an extended π-backbone generated from 1-ethynylpyrene (1-EP) appendages placed strategically in systematically varied sites. This was achieved synthetically through the selective bromination of the phen moiety and subsequent "on-the-complex" syntheses. The appropriately brominated phen was reacted with dichlorotetrakis(2-(2-pyridinyl)phenyl)diiridium(III), to generate the respective precursor mononuclear complexes. The 1-EP moieties were then attached via Sonogashira cross-coupling reactions to the 3-, 5-, 3,8- and 5,6-positions. The four novel Ir^{III} complexes formed in the successful cross-coupling reactions are presented in Scheme 1. The complexes including precursors were characterized by ^1H and ^{13}C NMR spectroscopy (Figures S1–S14 in the Supporting Information).

Their molecular masses were confirmed by mass spectrometry. Single crystals of **Ir-4** suitable for single-crystal X-ray analyses were obtained by the slow evaporation of

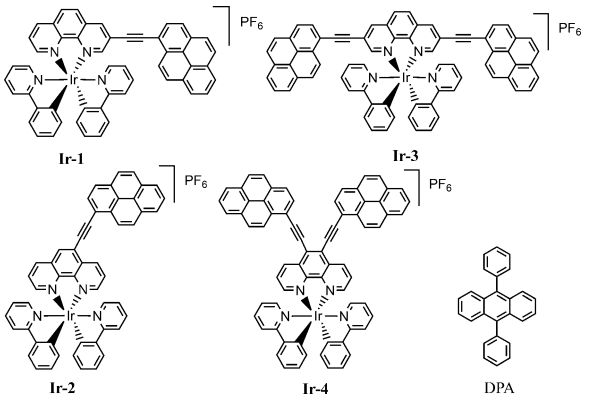

Scheme 1. Structures of the Ir^{III} complexes (**Ir-1**, **Ir-2**, **Ir-3** and **Ir-4**) as triplet photosensitizers and the triplet annihilator 9,10-diphenylanthracene (DPA).

a CH_2Cl_2 solution. Its molecular structure and relevant packing diagrams are presented in Figure S15.

The photophysical properties of each system were investigated (Table 1). The emissive states of **Ir-1**, **Ir-2** and **Ir-3** demonstrated long-lived excited state lifetimes at room temperature (RT). **Ir-4**, as the only complex exhibiting dual emission, had the lowest upconversion quantum yield of 7.9%. **Ir-2** exhibited an intermediate upconversion quantum yield ($\Phi_{UC} = 20.9\%$) and **Ir-1** and **Ir-3** had optimal upconversion quantum yields ($\Phi_{UC} = 30.2\%$ and 31.6%) (Table 2). To our knowledge, the latter are amongst the highest reported for Ir^{III} complexes upon excitation at a low power density.

Table 1: Photophysical data of Ir^{III} complexes.

	λ_{abs} [nm][a]	$\varepsilon \times 10^4$ [$M^{-1}cm^{-1}$][b]	λ_{em} [nm][a]	Φ_P [%][c]	τ_p [μs] (RT)
Ir-1	414/440	2.94/3.07	672/747	1.0	136.1[d]
Ir-2	410/434	3.01/2.86	678/751	0.1	213.1[d]
Ir-3	454/481	4.87/5.24	682/757	1.3	73.1[d]
Ir-4	445/485	2.82/2.45	600/738	0.5	1.3[e]/90.8[f]

[a] In CH_2Cl_2 (1×10^{-5} M). [b] Molar absorption coefficient. [c] Phosphorescence quantum yields, $[Ru(bpy)_3]\cdot 2PF_6$ in CH_3CN ($\Phi_P = 9.6\%$) was used as standard.[19] [d] Average lifetime value of the structured emission profile. [e] Fitted with monoexponential equation. [f] Fitted with biexponential equation ($1.5 \times 39\% + 147.9 \times 61\%$).

The UV-vis absorption spectra of the complexes are presented in Figure 1a. In all cases the absorptions in the region 250–350 nm are virtually superimposable with those observed in the combined spectra of the precursor Ir^{III} complex and free 1-EP. Significant new absorptions however are apparent in the visible region of the spectra. **Ir-1** displays a moderately intense absorption in the range of 414–441 nm. A similar profile is observed for **Ir-2** with the absorption maxima showing a small hypochromic shift (Table 1). In comparison, **Ir-4** shows a much broader absorption at $\lambda_{max}^{abs} = 445$ nm, due to the presence of an additional 1-EP unit. **Ir-3**, also containing two 1-EP groups exhibits significantly stronger and red-shifted absorptions in the visible range ($\lambda_{abs} = 481$ nm, $\varepsilon = 52{,}400\,M^{-1}cm^{-1}$). Overall, the visible absorptions of these Ir^{III} complexes have been successfully tuned by changing the number and position of their pyrene moieties.

Table 2: Photophysical properties of Ir^{III} complexes.[a]

	τ_T [μs][b]	K_{SV} (10^3) [M^{-1}][c]	k_q (10^9) [$M^{-1}s^{-1}$][d]	Φ_{UC} [%][e]
Ir-1	157.2	629.9	5.03	30.2
Ir-2	367.7	847.4	4.68	20.9
Ir-3	85.8	227.9	3.34	31.6
Ir-4	247.1	30.7	0.15	7.9

[a] In deaerated CH_2Cl_2 (1.0×10^{-5} M, 20 °C). [b] Triplet lifetime (τ_T). [c] Stern–Volmer quenching constants (K_{SV}). [d] Bimolecular quenching constants (k_q). [e] Upconversion quantum yields (Φ_{UC}).

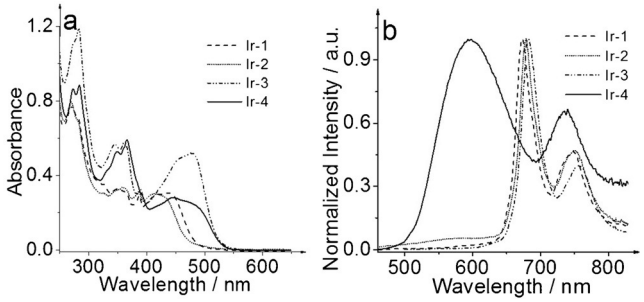

Figure 1. a) The UV-vis absorption spectra and b) normalized emission spectra of **Ir-1**, **Ir-2**, **Ir-3** and **Ir-4** in deaerated CH_2Cl_2 for comparison ($c = 1 \times 10^{-5}$ M, RT). $\lambda_{ex} = 440$ nm for **Ir-1**, **Ir-2** and **Ir-4**, and $\lambda_{ex} = 480$ nm for **Ir-3.**

The photoluminescence spectra were measured under an Ar atmosphere at RT. Normalized emission spectra are shown in Figure 1b. Significant vibrational progression is apparent. A peak centered at $\lambda_{em} = 672$ nm was observed for **Ir-1**, followed by a small shoulder at $\lambda_{em} = 747$ nm. Similar emission profiles were observed for **Ir-2** and **Ir-3**. Interestingly, although the absorption of **Ir-3** is much more intense than that of **Ir-1**, their T_1 energy levels (as indicated in their emission spectra) are very similar. This is an attractive result. It means that the structural changes have improved the absorption in the visible region, but also maintained a high T_1 energy level. Molecules in which the energy level at T_1 state is very low, are unlikely to have a practical use in TTA upconversion, as an appropriate triplet acceptor would be difficult to find.

In support of the photophysical analyses, TDDFT calculations (see later) showed that the spin density in **Ir-1**, **Ir-2** and **Ir-3** is not distributed across the entire molecule but only on the ligand, or as in **Ir-3,** part of the ligand. Long luminescence lifetimes (Table 1) were obtained for **Ir-1**, **Ir-2** and **Ir-3** ($\tau_p = 136.1$ μs, 213.1 μs and 73.1 μs, respectively at the chosen emission maxima), with **Ir-2** clearly possessing the longest. Unlike the other three Ir^{III} complexes, a highly blue-shifted emission peak at $\lambda_{em} = 600$ nm was observed for **Ir-4** (Figure 1b), which is typical of the ^{3}MLCT emission peak of Ir^{III} complexes in the literature. This peak is also accompanied by a small peak at a much longer wavelength ($\lambda_{em} = 738$ nm). Interestingly, the lifetimes of these two emissive states are independent of each other ($\lambda_{em} = 600$ nm, $\tau_p = 1.3$ μs; $\lambda_{em} = 738$ nm, $\tau_p = 90.8$ μs). Long lifetimes are generally indicative of radiative decay from ^{3}IL excited states, whilst shorter lifetimes usually suggest radiative decay from ^{3}MLCT excited states. Thus, we tentatively assign the emission of **Ir-1**, **Ir-2** and **Ir-3** to ^{3}IL, and the emissive states of **Ir-4** to a mix of ^{3}MLCT and ^{3}IL excited states. Low phosphorescence quantum yields were obtained for these Ir^{III} complexes, suggesting that the deactivation of the excited states is dominated by non-radiative processes.

The emission of **Ir-1**, **Ir-2** and **Ir-3** are effectively quenched when exposed to air (Figure S16). Although the emission of **Ir-4** at $\lambda_{em} = 737$ nm is totally quenched by air, the emission at $\lambda_{em} = 600$ nm did not show efficient quenching. This observation further suggests different characters for the two emission bands in **Ir-4** which were further investigated in terms of their solvent dependency and excitation wavelengths (Figure S18).

Low-temperature emission spectra at 77 K were also measured (Figure S17). Small hypochromic shifts were observed for **Ir-1** (73.2 cm^{-1}), **Ir-2** (198.4 cm^{-1}) and **Ir-3** (196.1 cm^{-1}) when compared to the emission spectra at RT.

For **Ir-4**, the emission at $\lambda_{em} = 600$ nm shows a large Stokes shift (ΔE_s, 628.4 cm^{-1}), while the emission at $\lambda_{em} = 738$ nm disappears. This may be due to the decreased polarity of the frozen glass, or due to the thermal inaccessibility of the ^{3}IL energy level. A similar phenomenon has been previously observed for pyrene-containing Ru^{II} complexes.[16] A large ΔE_s value typically indicates ^{3}MLCT emissive states, whereas a small ΔE_s suggests ^{3}IL emissive states.[17–18] In summary we attribute ^{3}IL character to the excited states in **Ir-1**, **Ir-2** and **Ir-3**, and mixed ^{3}MLCT and ^{3}IL character to those of **Ir-4**.

In nanosecond time-resolved absorption studies, **Ir-1** and **Ir-2** show similar profiles with bleaching peaks around 410 nm (Figure S19) due to ground-state depletion. Transient absorption is detected in all complexes above 460 nm. As expected the populated triplet excited states upon excitation were determined as ^{3}IL, however **Ir-3** and **Ir-4** show some superposition of their bleaching bands and excited-state absorption bands. These eventually form quite different transients (Figure 2). **Ir-3** displays two significant bleaching peaks at

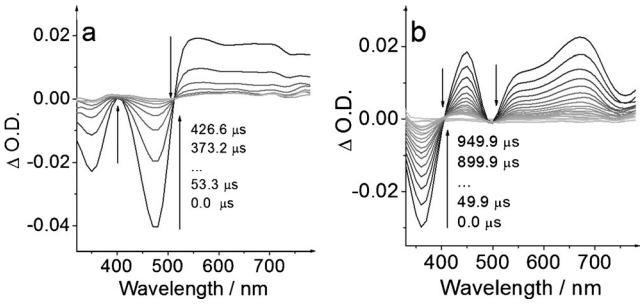

Figure 2. Nanosecond time-resolved transient difference absorption spectra of a) **Ir-3** ($\lambda_{ex} = 481$ nm) and b) **Ir-4** ($\lambda_{ex} = 434$ nm), in deaerated CH_2Cl_2, RT.

350 and 480 nm followed by transient absorption above 515 nm. The first two features ($\lambda = 350$ nm and $\lambda = 480$ nm) are in agreement with the absorption spectrum of **Ir-3** (Figure 1). The transient absorption over 515 nm is characteristic of the ligand-localized T_1 excited state. Intense bleaching is also observed at shorter wavelengths ($\lambda = 360$ nm), along with two transient absorption peaks at longer wavelength ($\lambda =$ 450 and 670 nm) in **Ir-4**. We therefore propose that the earlier assignment of the emissive states of **Ir-4** to a mix of ^{3}MLCT and ^{3}IL emissive states to be appropriate (Figure S20).

TDDFT calculations were carried out to rationalize the photophysical properties of the four Ir^{III} complexes. The HOMO (H) of the four Ir^{III} complexes are found to be mainly localized on the pyrene units (Figure S22). In contrast, the LUMO (L) resides on the 1,10-phenanthroline moiety in all cases. The calculated UV-vis absorption is in good agreement with the experimental results (Table S1). The S_1 in **Ir-1** originates from H-1→L and H-1→L + 2, but the intensity of the state is very weak ($f = 0.0075$). The S_2 results from H→L excitation which implies a intra-ligand charge transfer (IL) from the pyrene moiety to the central 1,10-phenanthroline unit. **Ir-2** and **Ir-4** have their lowest singlet excited states from H→L, which can be ascribed to *IL. This is not observed for **Ir-3**, where the S_1 state was assigned as having both ^{1}MLCT (H-2→L) and ^{1}IL (H→L) character.

The lowest-lying triplet states (T_1) of all the complexes result from a mixing of pyrene→phen and pyrene→pyrene excitations. In line with the photophysical studies, the TDDFT calculations indicate that the lowest-energy emissions in the four Ir^{III} complexes take place from triplet states localized on the large coordinating ligands. These results were further supported by the spin-density surfaces of the triplet states of the complexes (Figure 3). The spin density is found

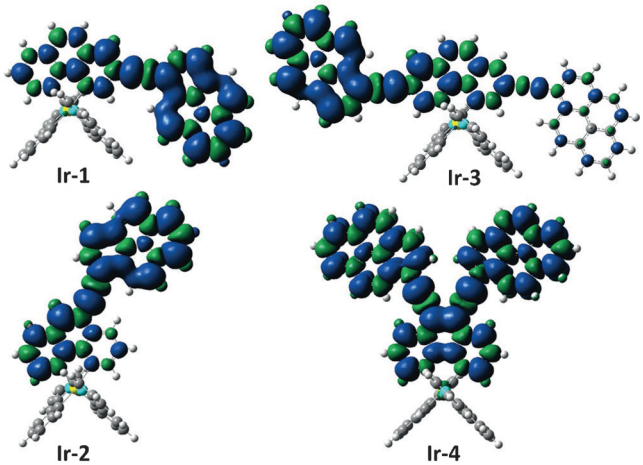

Figure 3. Spin density distribution of the lowest triplet state of arrays **Ir-1**, **Ir-2**, **Ir-3** and **Ir-4**. Calculated at the DFT/PBEH1PBE/6-31(g)/LANI2DZ level with Gaussian 09W.

to be distributed equally across both pyrene and phen in **Ir-1** and **Ir-2**. In **Ir-3**, it is mainly confined to the central 1,10-phenanthroline and one pyrene unit, which may explain its similar ^{3}IL energy level to **Ir-1**. The contribution of the metal center and coordinated phenylpyridine (ppy) ligands appears to be minimal in these three complexes. In the case of **Ir-4**, however where the two 1-EP are in the 5,6- as opposed to the 3,8-positions on the coordinated phen, the spin density is distributed through the Ir^{III} center and across the entire phen ligand. Here the contribution from both pyrene units to the 1,10-phenanthroline center dominates the spin density calculation and due to the increased electron delocalization effects, the energy gap between H and L is narrowed. This is most likely to be due to a lowering of the L energy, an effect that is seen in the emission from ^{3}IL appearing at a much longer wavelength.

Strong absorption in the visible region, coupled with long-lived triplet excited state lifetimes make these Ir^{III} complexes potential candidates as triplet photosensitizers for TTA upconversion. 9,10-Diphenylanthracene (DPA) was selected as an appropriate triplet annihilator due to its high fluorescence quantum yield (95% in ethanol) and the position of its lowest-lying triplet energy level (1.77 eV). All of the complexes were excited at $\lambda_{ex} = 473$ nm under a 70.3 mW cm^{-2} power density laser excitation. The resulting upconverted fluorescence can be observed by the naked eye (Figure 4 and Figure S20).

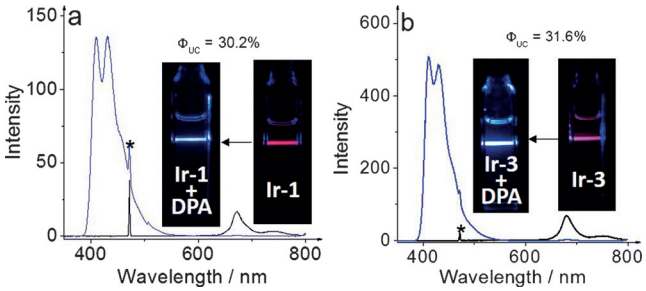

Figure 4. Upconversion spectra of **Ir-1** and **Ir-3** as triplet sensitizers in the presence of DPA (blue) and emission spectra of Ir^{III} complexes alone (black). The insets show photographs of triplet sensitizers with DPA and without DPA. λ_{ex} = 473 nm, 70.3 mW cm^{-2}, in deaerated CH_2Cl_2, RT.

Ir-1 and **Ir-3** show similar high upconversion quantum yields of 30.2 % (DPA: 6 equiv) and 31.6 % (DPA: 14 equiv), respectively. The results were repeated and confirmed. Complexes with such high upconversion efficiency are rarely observed in the literature. For **Ir-2**, efficient upconversion was also observed (Φ_{UC} = 20.9 %; DPA: 6 equiv) (Figure S21). We propose that the long ^{3}IL triplet lifetimes significantly contribute to the high upconversion quantum yields observed for each of the complexes **Ir-1**, **Ir-2** and **Ir-3**. For **Ir-4**, a much lower upconversion quantum yield was obtained even in the presence of considerable amounts of DPA (20 equiv) (Φ_{UC} = 7.9 %). Although **Ir-4** also posseses a long-lived ^{3}IL excited state, the energy level of the lowest-lying ^{3}IL excited state is calculated as 1.68 eV, which is lower than that of the T_1 energy level of DPA (1.77 eV). Most probably this results in the triplet–triplet energy transfer (TTET) process being less efficient. This supposition is supported by the fact that the phosphorescence lifetime of the higher ^{3}MLCT energy emissive (2.07 eV) is quite short.

The validity of these results were further examined quantitatively by the quenching of the phosphorescence of the Ir^{III} complexes with DPA. By detecting the triplet lifetime of each Ir^{III} complex after each addition of DPA, the Stern–Volmer quenching plots were obtained (Figure 5).

In each case, quenching by Föster energy transfer was not found. This is most likely due to unmatched excited state

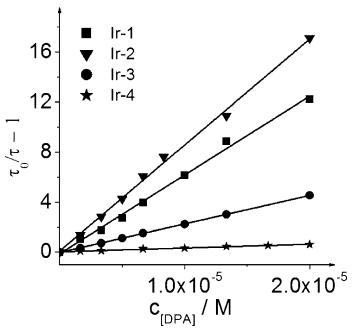

Figure 5. Stern–Volmer plots generated from quenching lifetime of **Ir-1** (λ_{ex} = 420 nm), **Ir-2** (λ_{ex} = 416 nm), **Ir-3** (λ_{ex} = 481 nm) and **Ir-4** (λ_{ex} = 434 nm) measured as a function of DPA (triplet quencher) concentration in CH_2Cl_2, RT.

energy levels between donor and acceptor in solution. The TTET processes are attributed therfore as being the result of Dexter energy transfer. Sensitizers with extended excited state lifetimes usually generate an increased probability of encounter with the acceptor molecule, resulting in a more efficient TTET process.

Ir-1, **Ir-2** and **Ir-3** gave optimal Stern–Volmer quenching constants, with **Ir-2** demonstrating the most significant quenching effect ($K_{SV=}847.4\times10^3\,M^{-1}$) in the presence of DPA (Table 2). This result is in good agreement with the trend in the triplet excited state lifetimes of the complexes. Although **Ir-2** has a much longer lifetime and also a higher K_{SV} value, it possesses a slightly lower upconversion quantum yield which we attribute to its weaker absorption at the excitation wavelength compared to **Ir-1** and **Ir-3**.

The bimolecular quenching constants were calculated giving very similar values for each Ir^{III} complex however, as expected **Ir-4** clearly displays the lowest quenching constant. Although the triplet lifetime of **Ir-4** is quite long, the unmatched T_1 energy levels of **Ir-4** and DPA are resulting in an inefficient TTET process.

In conclusion, Ir^{III} complexes based on pyrene-functionalized 1,10-phenanthrolines (phen) were successfully synthesised via a "chemistry-on-the-complex" method. Tunable visible absorption and emission wavelengths were achieved by controlling the number and the position of the pyrene moieties. Structured emission profiles were observed for **Ir-1**, **Ir-2** and **Ir-3.** These are the Ir^{III} phen complexes with 1-ethynylpyrene (1-EP) in 3-, 5- and 3,8-positions, respectively. Their long-lived ^{3}IL excited states were studied. The T_1 excited states were confirmed by nanosecond time-resolved transient absorption spectra and DFT calculations. A comparison between 3,8- and 5,6-substituted phen complexes, **Ir-3** and **Ir-4,** show that these triplet lifetimes are regioisomer-specific. Unusually dual emission was observed for the 5,6-substituted **Ir-4**, and could be attributed to radiative decay from both ^{3}MLCT and ^{3}IL excited states. TTA upconverted blue fluorescence in the presence of DPA was observed for **Ir-4** (Φ_{UC} = 7.9 %), **Ir-1** (Φ_{UC} = 30.2 %), **Ir-2** (Φ_{UC} = 20.9 %) and **Ir-3** (Φ_{UC} = 31.6 %). The upconversion quantum yields of **Ir-1** and **Ir-3** are, to the best of our knowledge, the highest reported to date for Ir^{III} complexes when excited using a low-power density laser.

The introduction of a second 1-EP at the 8-position of the phen (**Ir-3** compared to **Ir-1**) gave rise to more intensive absorption in the visible region without decreasing the T_1 energy level. This result, along with the outstanding upconversion quantum yields, offers promise in the search for triplet photosensitizers with the potential for practical application in photovoltaics and photocatalysis.

Experimental Section

General methods for the syntheses, structural, optical and electrochemical characterizations of the numbered compounds are available in the Supporting Information. CCDC 1501155 (**Ir-4**) contains the supplementary crystallographic data for this paper. These data can be obtained free of charge from The Cambridge Crystallographic Data Centre.

Acknowledgements

We thank Drs J. O'Brien, M. Reuther, M. Feeney and G. Hessman for spectroscopic and technical assistance. This material is based upon works supported by the Science Foundation Ireland under Research Grant Nos SFI/09/IN.I/12974, SFI/15/1A/3046 and SFI Walton Award 11/W.1/E2061. Y.L. and J.W. acknowledge PG studentships from the School of Chemistry and the Irish Research Council, respectively.

Keywords: iridium(III) · phenanthroline · pyrene · triplet–triplet annihilation · upconversion

How to cite: *Angew. Chem. Int. Ed.* **2016**, *55*, 14688–14692
Angew. Chem. **2016**, *128*, 14908–14912

[1] J. C. Goldschmidt, S. Fischer, *Adv. Opt. Mater.* **2015**, *3*, 510–535.
[2] Y. Y. Cheng, A. Nattestad, T. F. Schulze, R. W. MacQueen, B. Fückel, K. Lips, G. G. Wallace, T. Khoury, M. J. Crossley, T. W. Schmidt, *Chem. Sci.* **2016**, *7*, 559–568.
[3] V. Gray, D. Dzebo, M. Abrahamsson, B. Albinsson, K. Moth-Poulsen, *Phys. Chem. Chem. Phys.* **2014**, *16*, 10345–10352.
[4] C. Wohnhaas, V. Mailander, M. Droge, M. A. Filatov, D. Busko, Y. Avlasevich, S. Baluschev, T. Miteva, K. Landfester, A. Turshatov, *Macromol. Biosci.* **2013**, *13*, 1422–1430.
[5] Q. Liu, T. Yang, W. Feng, F. Li, *J. Am. Chem. Soc.* **2012**, *134*, 5390–5397.
[6] Q. Liu, W. Feng, T. Yang, T. Yi, F. Li, *Nat. Protoc.* **2013**, *8*, 2033–2044.
[7] R. S. Khnayzer, J. Blumhoff, J. A. Harrington, A. Haefele, F. Deng, F. N. Castellano, *Chem. Commun.* **2012**, *48*, 209–211.
[8] C. Ye, J. Wang, X. Wang, P. Ding, Z. Liang, X. Tao, *Phys. Chem. Chem. Phys.* **2016**, *18*, 3430–3437.
[9] J. Zhao, W. Wu, J. Sun, S. Guo, *Chem. Soc. Rev.* **2013**, *42*, 5323–5351.
[10] L. Ma, H. Guo, Q. Li, S. Guo, J. Zhao, *Dalton Trans.* **2012**, *41*, 10680–10689.
[11] W. Zhao, F. N. Castellano, *J. Phys. Chem. A* **2006**, *110*, 11440–11445.
[12] J. Sun, F. Zhong, X. Yi, J. Zhao, *Inorg. Chem.* **2013**, *52*, 6299–6310.
[13] P. Duan, N. Yanai, N. Kimizuka, *Chem. Commun.* **2014**, *50*, 13111–13113.
[14] J. Wang, Y. Lu, N. McGoldrick, C. Zhang, W. Yang, J. Zhao, S. M. Draper, *J. Mater. Chem. C* **2016**, *4*, 6131–6139.
[15] Y. Lu, N. McGoldrick, F. Murphy, B. Twamley, X. Cui, C. Delaney, G. M. Maille, J. Wang, J. Zhao, S. M. Draper, *Chem. Eur. J.* **2016**, *22*, 11349–11356.
[16] A. Harriman, A. Khatyr, R. Ziessel, *Dalton Trans.* **2003**, 2061–2068.
[17] H. Guo, M. L. Muro-Small, S. Ji, J. Zhao, F. N. Castellano, *Inorg. Chem.* **2010**, *49*, 6802–6804.
[18] H. Sun, H. Guo, W. Wu, X. Liu, J. Zhao, *Dalton Trans.* **2011**, *40*, 7834–7841.
[19] W. Wu, J. Sun, X. Cui, J. Zhao, *J. Mater. Chem. C* **2013**, *1*, 4577–4589.

Received: August 29, 2016
Published online: October 20, 2016

